

Lorentz angle in the ATLAS pixel detector: Effects of operating parameters and radiation damage

Javier Llorente,
on behalf of the ATLAS Collaboration

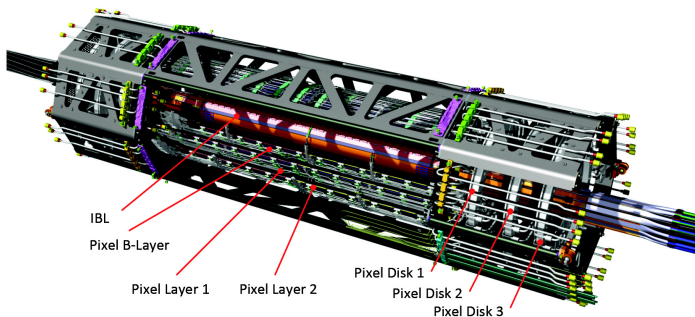
IHEP Beijing

Workshop on Advanced Silicon Radiation Detectors
February 25, 2019



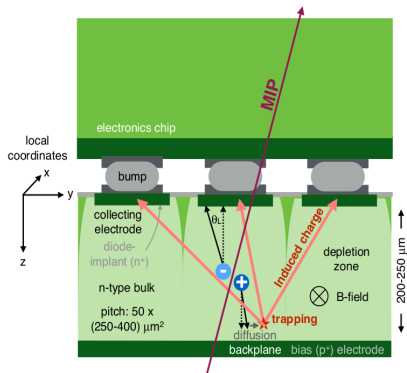
- The ATLAS pixel detector and radiation damage digitizer.
- Definition and properties of the Lorentz angle.
- Measurement strategy and fit definition.
- Measurements with cosmic muons in Run I. Temperature dependence.
- Radiation damage after Run I: Results with cosmic muons.
- Electron and hole mobility models.
 - Low-field parameterisations of $\mu(T)$.
 - High-field extrapolations. The extended Thomas model.
- Radiation damage on Run II: IBL Lorentz angle in pp collisions.
- Simulation: Chiochia model and ATLAS radiation damage digitizer.
- Summary and conclusions.

The ATLAS pixel detector is composed of four layers and three endcap disks



Layer	$\langle r \rangle$ [mm]	Staves	Modules	Channels	Disk	$\langle z \rangle$ [mm]	Sectors	Modules	Channels
0	33.3	14	224	6.02×10^6	0	495	8	48	2.2×10^6
1	50.5	22	286	13.2×10^6	1	580	8	48	2.2×10^6
2	88.5	38	494	22.8×10^6	2	650	8	48	2.2×10^6
3	122.5	52	676	31.2×10^6					

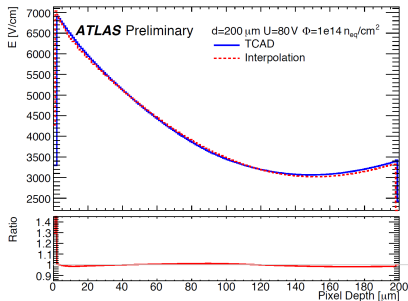
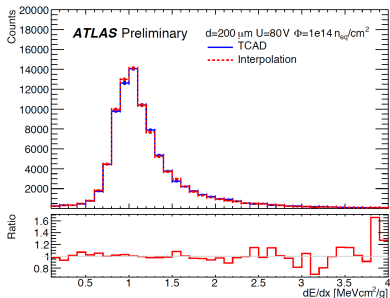
Signal digitization is done using the ATHENA framework interfaced with G4.



- Simulation takes energy and position of MIP as inputs.
- Ionization energy converted into electrons and holes (~ 3.65 eV/pair)
- Charges suffer thermal diffusion and drifts in \vec{E} , \vec{B} fields.
- Charge trapping is randomly set, by comparing trapping time (Φ -dependent) with drift time.

After digitization, the collected charge in each module is read out.

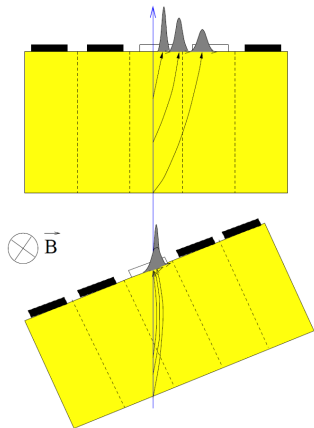
- Electric field is calculated by interpolation from benchmark simulations.
- Simulations use TCAD maps for a given voltage and fluence.
- Irradiated sensors with non-linear profiles simulated using Chiochia model.
- Interpolation is done using cubic splines in both dimensions (V , Φ)
- Closure of the interpolation and TCAD simulation is shown below



Very good closure observed between the simulated and interpolated results.

Lorentz angle: Definition and properties

Lorentz Angle: angle of deviation of drifting electrons in the Si modules under the effect of the solenoidal magnetic field



- Cluster transverse size is a function of the incidence angle φ .
- With $\vec{B} \neq 0$, the cluster size has a minimum for $\varphi = \theta_L$.
- Knowledge of θ_L can be used to improve spatial resolution.
- Important for understanding mobility models in Monte Carlo.
- Indicator of radiation damage.

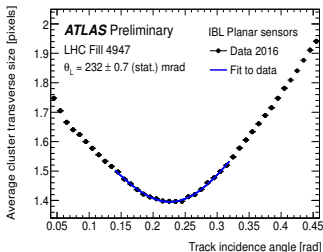
- Tracks with hits in the pixel detector are selected for the analysis.
- Cluster size is presented as a function of the incidence angle in $R\phi$ plane.
- The distributions are fitted to the following function

$$W(\varphi) = \left(a |\tan \varphi - \tan \theta_L| + \frac{b}{\sqrt{\cos \varphi}} \right) \otimes G(\varphi),$$

where \otimes is the convolution. The free parameters are a , θ_L , b and σ :

- $a \equiv$ Related to the depletion depth.
- $\theta_L \equiv$ The Lorentz angle.
- $b \equiv$ The minimum cluster size.
- $\sigma \equiv$ The resolution on the incidence angle.

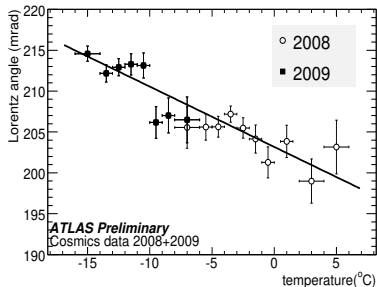
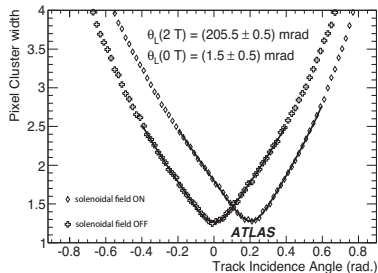
IBL, LHC Fill 4947



First measurements with cosmic muons (2008-2009)

Lorentz angle from cosmic muons [arXiv:1004.5293]

- Fixed conditions: $V = -150$ V, $T = -3$ °C.
- Temperature scan keeping $V = -150$ V.



Measured dependence with T: $\frac{\partial \theta_L}{\partial T} = (-0.74 \pm 0.03)$ mrad/K

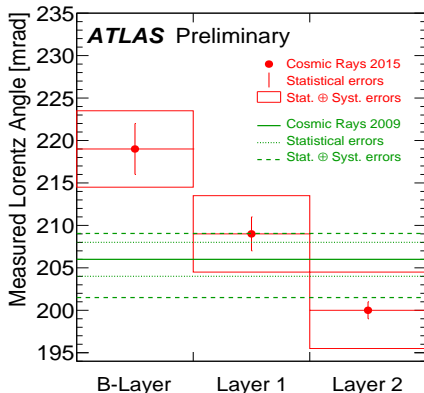
Predicted dependence with T: $\frac{\partial \theta_L}{\partial T} = -0.74$ mrad/K

[C. Jacoboni *et al.*: Solid State Electronics 20, 77 (1977)]

Lorentz angle in cosmic muons (2015)

Lorentz angle in cosmic data taken in two different periods (IDTR-2017-002)

- Cosmics 2009: Inclusively in all layers.
- Cosmics 2015: Separated in three layers (L1 and L2 compatible with 2009)



- Same temperature and voltage conditions: $T = -10\text{ }^{\circ}\text{C}$, $V = -150\text{ V}$.
- After Run-I, B-layer received more radiation than L1, L2 \Rightarrow Larger θ_L

- Equivalent to modelling the mobility μ ($\tan \theta_L \sim \mu |\vec{B}|$).
- 10% discrepancy found in Run I: [ATL-INDET-PUB-2018-001](#)
- Mobility $\mu(T, \vec{E})$ defines the drift velocity: $\vec{v}_d = \mu \vec{E}$.
- Parameterisations of electron and hole low and high-field mobility:
 - Low-field mobility parameterised by a power law:

$$\mu(T) = a T_n^{-b}; \quad T_n = \frac{T}{300 \text{ K}}$$

- High-field mobility extrapolated using [Thomas parameterisation](#)

$$\mu(T, E) = \mu_0(T) \left[1 + \left(\frac{\mu_0(T) E}{\nu_s(T)} \right)^\beta \right]^{-\frac{1}{\beta}}$$

For low electric field, three main models are studied

- Jacoboni-Canali:

$$\mu_{e,0}(T) = 1533.7 \text{ cm}^2/(\text{V} \cdot \text{s}) T_n^{-2.42}$$

$$\mu_{h,0}(T) = 463.9 \text{ cm}^2/(\text{V} \cdot \text{s}) T_n^{-2.20}$$

- Canali:

$$\mu_{e,0}(T) = 1437.7 \text{ cm}^2/(\text{V} \cdot \text{s}) T_n^{-2.42}$$

$$\mu_{h,0}(T) = 463.9 \text{ cm}^2/(\text{V} \cdot \text{s}) T_n^{-2.20}$$

- Hamburg-Thomas

$$\mu_{e,0}(T) = 1440(15) \text{ cm}^2/(\text{V} \cdot \text{s}) T_n^{-2.260(7)}$$

$$\mu_{h,0}(T) = 474(10) \text{ cm}^2/(\text{V} \cdot \text{s}) T_n^{-2.619(7)}$$

High-field mobility is extrapolated using

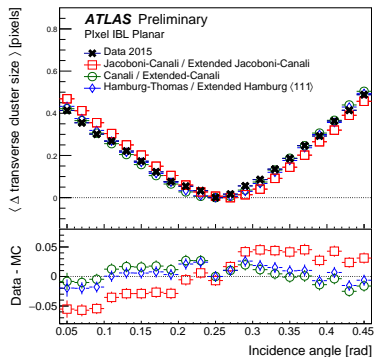
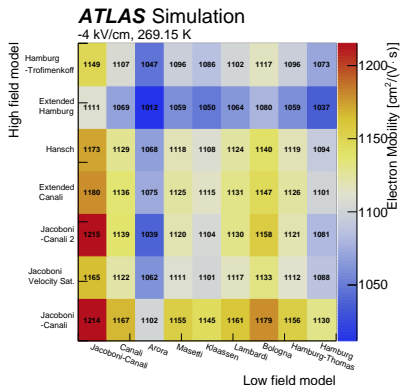
$$\mu(T, E) = \mu_0(T) \left[1 + \left(\frac{\mu_0(T)E}{\nu_s(T)} \right)^\beta \right]^{-\frac{1}{\beta}}$$

The expressions of ν_s and β for electrons and holes are given below

Extended Model	Parameter	Electrons	Holes
Jacoboni-Canali	ν_s (cm/s)	$1.07 \times 10^7 \times T_n^{-0.87}$	$8.34 \times 10^6 \times T_n^{-0.52}$
	β	$1.109 \times T_n^{0.66}$	$1.213 \times T_n^{0.17}$
Canali	ν_s (cm/s)	$1.00 \times 10^7 \times T_n^{-0.87}$	$8.34 \times 10^6 \times T_n^{-0.52}$
	β	$1.109 \times T_n^{0.66}$	$1.213 \times T_n^{0.17}$
Hamburg	ν_s (cm/s)	$1.054(38) \times 10^7 \times T_n^{-0.602(3)}$	$9.40(27) \times 10^6 \times T_n^{-0.226(2)}$
	β	$0.992(4) \times T_n^{0.572(3)}$	$1.181 \times T_n^{0.644(3)}$

Mobility models confronted to IBL data

- Mobility at 80 V and $-4\text{ }^{\circ}\text{C}$ predicted by many different models (left)
- Description of the data made by the three models under discussion (right)

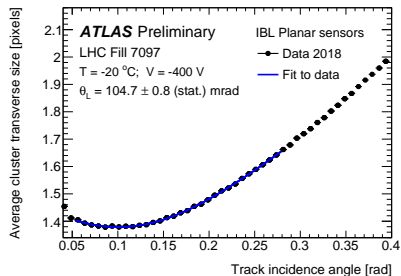
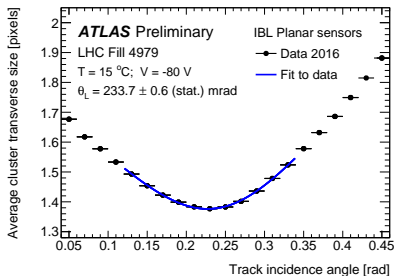


Canali / Extended Canali model is used for Run-II simulation and beyond.

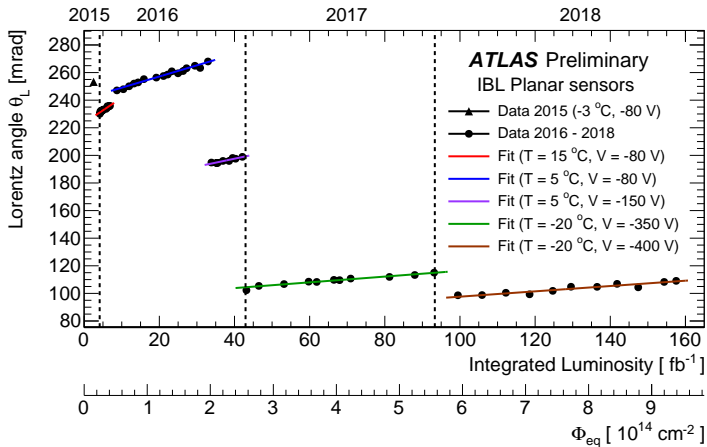
Measurement of the IBL Lorentz angle over Run II

- Measurements of θ_L performed over Run II as a function of the luminosity.
- Different periods with different temperature and voltage conditions .

Year	Bias voltage [V]	Temperature [°C]	Luminosity [fb^{-1}]
2015	-80	-3	4.1
2016	-80	+15	3.0
	-80	+5	26.2
2017	-150	+5	9.6
	-350	-20	50.4
2018	-400	-20	64.2



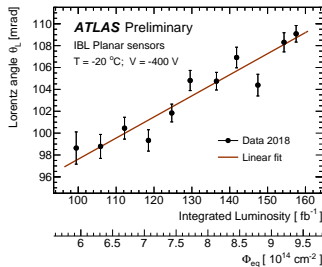
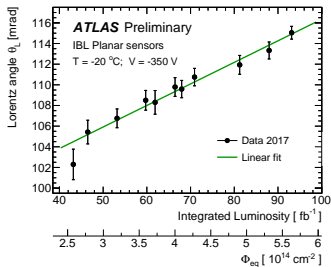
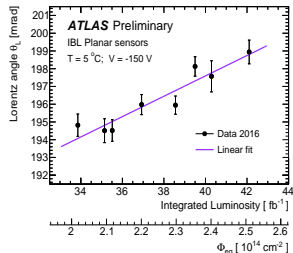
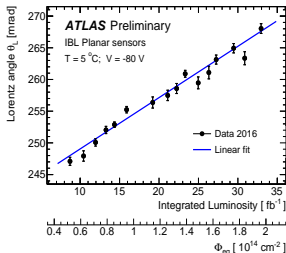
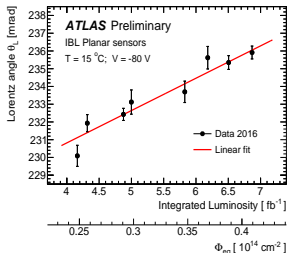
Lorentz angle evolution over Run II



- Linear, increasing trend with $\mathcal{L} \propto \Phi_{\text{eq}}$ observed in each period.
- Value of θ_L increases when decreasing temperature.
- Value of θ_L decreases when increasing voltage.
- Slope is milder with increasing voltage (decreasing temperature)

Lorentz angle evolution over Run II

Detailed variation of θ_L for each separate period

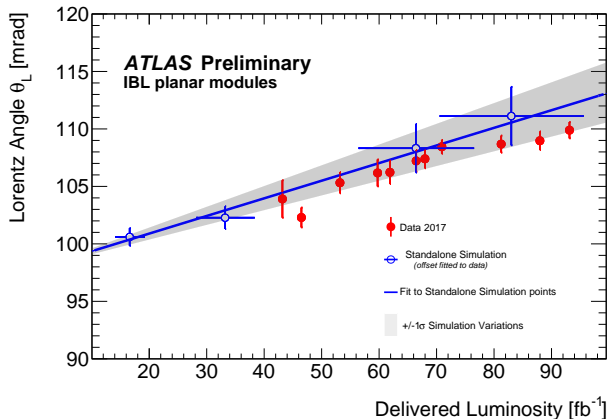


Results of the linear fits to each period are summarised below

Temperature	Voltage	$\theta_L(\Phi_{\text{eq}} = 0)$ [mrad]	$(\partial\theta_L/\partial\Phi_{\text{eq}})_{T,V}$ [mrad · cm ²]
15 °C	80 V	223.5 ± 1.0	$(30.6 \pm 3.0) \cdot 10^{-14}$
5 °C	80 V	240.9 ± 0.7	$(13.6 \pm 0.6) \cdot 10^{-14}$
	150 V	174.6 ± 3.6	$(9.6 \pm 1.6) \cdot 10^{-14}$
-20 °C	350 V	95.5 ± 1.3	$(3.5 \pm 0.3) \cdot 10^{-14}$
	400 V	78.3 ± 2.8	$(3.2 \pm 0.4) \cdot 10^{-14}$

- Lorentz angle at zero fluence increases with decreasing temperature.
- Lorentz angle at zero fluence decreases with increasing voltage.
- Radiation damage degradation milder for lower temperatures.
- Radiation damage degradation milder for higher voltages.

Chiochia model is used as input to ATLAS radiation damage digitizer.



- Vertical error bars on data are the fit results.
- Slope is fitted to the simulation, while offset is fitted from data.
- Grey uncertainty band: statistical and systematic (simulation parameters).
- Horizontal error bars: luminosity to fluence conversion.

- Measurements and simulations of the Lorentz angle have been presented.
- Hints of radiation damage on *B*-Layer observed in cosmic data after Run I.
- Different mobility models have been investigated.
- Best description by Canali + Extended Canali model, used from now on.
- Measurements of the Lorentz angle as a function of the fluence presented.
- Good description of the effects by the Chiochia model is observed.